JACC: ADVANCES VOL. 3, NO. 11, 2024

ORIGINAL RESEARCH

Flow Dynamic Factors Correlated With Device-Related Thrombosis After Left Atrial Appendage Occlusion

Brennan J. Vogl, BS,[a] Emily Vitale, BS,[a] Sunyoung Ahn, MS,[a] Agata Sularz, MB BCHIR,[b] Alejandra Chavez Ponce, MD,[b] Gerardo V. Lo Russo, MD,[b] Jeremy Collins, MD,[c] Alessandra Maria Bavo, PHD,[d] Ahmed El Shaer, MD,[b] Anders Kramer, MD,[e] Yuheng Jia, MD,[f] Davorka Lulic, MD,[f] Matthieu De Beule, PHD,[d] Jens Erik Nielsen-Kudsk, MD,[e] Ole De Backer, MD,[f] Mohamad Alkhouli, MD,[b,*] Hoda Hatoum, PHD[a,g,*]

ABSTRACT

BACKGROUND Device-related thrombosis (DRT) occurs in up to 4% of patients undergoing left atrial appendage occlusion (LAAO) and is associated with substantial morbidity and mortality. However, its pathophysiology, predictors, and optimal management remain unclear.

OBJECTIVES This study aims to assess flow dynamic factors correlating to DRT.

METHODS A multicenter registry of patients who underwent LAAO and had pre- and post-computed tomography imaging was used. Patient-specific 3-dimensional digital models of the left atrium were created, and finite element simulations were performed to implant an LAAO device into each model in a position that matched the clinical deployment. Computational fluid dynamic simulations were performed to quantify the following flow dynamic parameters: time averaged wall shear stress, oscillatory shear index, and endothelial cell activation potential.

RESULTS A total of 38 patients (19 with DRT and 19 without DRT) were included. Left atrium volumes and mitral valve areas were larger in the DRT cohort compared with controls. Patients with DRT had a significantly lower time averaged wall shear stress (1.76 $\pm$ 1.24 Pa vs 2.90 $\pm$ 2.70 Pa), a higher oscillatory shear index (0.19 $\pm$ 0.11 vs 0.17 $\pm$ 0.11), and a higher endothelial cell activation potential (0.23 $\pm$ 0.58 Pa^{-1} vs 0.17 $\pm$ 0.30 Pa^{-1}) than the controls ($P < 0.001$ for all). Thrombus locations identified from in-vivo images correlated well with the flow dynamic parameters tested.

CONCLUSIONS Flow dynamic parameters may be able to predict the risk of DRT after LAAO. Further investigation with a larger patient cohort and long-term follow-up is needed to assess the role of computational fluid dynamics in the risk stratification of patients considered for LAAO. (JACC Adv. 2024;3:101339) © 2024 The Authors. Published by Elsevier on behalf of the American College of Cardiology Foundation. This is an open access article under the CC BY-NC-ND license (http://creativecommons.org/licenses/by-nc-nd/4.0/).

From the [a]Department of Biomedical Engineering, Michigan Technological University, Houghton, Michigan, USA; [b]Department of Cardiovascular Medicine, Mayo Clinic, Rochester, Minnesota, USA; [c]Department of Radiology, Mayo Clinic, Rochester, Minnesota, USA; [d]FEops NV, Gent, Belgium [e]Department of Cardiology, Aarhus University Hospital, Aarhus, Denmark; [f]Department of Cardiology, Copenhagen University Hospital, Copenhagen, Denmark; and the [g]Health Research Institute, Center of Biocomputing and Digital Health and Institute of Computing and Cybersystems, Michigan Technological University, Houghton, Michigan, USA. *Drs Alkhouli and Hatoum are co-senior authors.

The authors attest they are in compliance with human studies committees and animal welfare regulations of the authors' institutions and Food and Drug Administration guidelines, including patient consent where appropriate. For more information, visit the Author Center.

Manuscript received July 12, 2024; revised manuscript received September 12, 2024, accepted September 15, 2024.

ISSN 2772-963X https://doi.org/10.1016/j.jacadv.2024.101339

ABBREVIATIONS AND ACRONYMS

BCs = boundary condition

CFD = computational fluid dynamics

CT = computed tomography

DRT = device-related thrombosis

ECAP = endothelial cell activation potential

LA = left atrium

LAA = left atrial appendage

LAAO = left atrial appendage occlusion

OSI = oscillatory shear index

MV = mitral valve

TAWSS = time averaged wall shear stress

WSS = wall shear stress

Atrial fibrillation is the most common arrhythmia affecting over 10 million individuals in the United States alone.[1] Stroke prevention remains a major concern in the management of atrial fibrillation.[2,3] While anticoagulants are effective in mitigating strokes, bleeding risk, noncompliance, and other side effects preclude their consistent use in >50% of eligible patients.[3,4] To address this unmet need, left atrial appendage (LAA) occlusion (LAAO) emerged as an alternative approach to prevent potential strokes.[5] The efficacy of LAAO has been documented in several randomized trials and a large body of observational studies, leading to a growing adoption in clinical practice. A previous computational study by our group evaluated the efficacy of LAAO.[6] However, certain unresolved issues with the therapy remain, including device related thrombosis (DRT).[7-10] DRT occurs in 3% to 5% of patients undergoing LAAO and is associated with a 4-fold increase in cardioembolic events.[7-12] Furthermore, the treatment of DRT is challenging with a high frequency of persistence, bleeding risk, and recurrence rates.[13] Therefore, considerable efforts have been made to identify risk factors for DRT.[14]

Given the close relationship between thrombosis and flow stasis, there has been a growing interest in investigating flow dynamics associated with DRT using computational fluid dynamics (CFD) techniques.[15-17] However, studies assessing CFD correlates of DRT have been hindered by their small size and lack of a control group.[18-20] To bridge this gap, we combined patient-specific CFD analyses with finite element simulations in a larger sample of patients with and without DRT from multiple institutions.

This study aims to characterize the fluid dynamic environment around LAAO devices in attempt to assess the flow dynamic factors correlating to DRT.

METHODS

PATIENT DATA. This retrospective study used a database of 38 patients who underwent LAAO procedure from Mayo Clinic (Rochester, Minnesota, USA), Aarhus University Hospital (Aarhus, Denmark), and Copenhagen University Hospital (Copenhagen, Denmark) of which 19 developed DRT and 19 did not (control). All DRTs were verified by 2 separate expert cardiologists. Patient characteristics are shown in Table 1. The patient data sets included preprocedural and postprocedural computed tomography (CT) scans and echocardiographic waveforms. This study was performed under an approved Institutional Review Board protocol and data usage agreement between Michigan Technological University, Mayo Clinic, Aarhus, and Copenhagen University Hospitals.

DIGITAL 3-DIMENSIONAL MODEL DEVELOPMENT. The workflow adopted in this study is shown in Figure 1. CT images of patients with and without DRT after LAAO were imported into Mimics Research 23.0 (Materialise) for processing. A mask (using a threshold that isolates blood from soft tissue) was applied to the CT images and segmentation was performed to create a patient-specific 3-dimensional digital model of the left atrium (LA) and LAA. The mitral valve (MV) was segmented as a saddle shaped opening and the pulmonary veins were cut at their ostia. Finite-element computational simulations were performed by FEops NV to deploy an LAAO device into each model in a position that matched the postprocedural CT positioning for each patient (Supplemental Figure 1).[21] The output of the finite element analysis simulations, that is, the patient-specific anatomy deformed after the virtual deployment of the LAA device and the device itself, were retained and used as input for the CFD simulations. The novelty of this technique is twofold: 1) an accurate model of the device as seen in postprocedural imaging is virtually deployed in the atrium models as opposed to merely creating a sealing surface at the LAA ostium,[22] which accounts for the potential presence of peri-device leak paths, and 2) the walls at the region of the deployment are deformed as the device is expanded into position, accurately depicting real-world device deployment. Thrombi identified in in-vivo imaging were not included in the digital models, thus simulating the device-related flow environment immediately after deployment. Geometric measurements were recorded for LA volumes, MV areas, and thrombus volumes.

COMPUTATIONAL FLUID DYNAMICS. The digital models (after virtual device deployment) were imported into Ansys Workbench 2020 R1 for the CFD simulations. Prior to that, extensions equivalent to ten times the atrial inlets and outlet diameters were created to overcome entrance effects and to have an appropriate velocity profile.[23] An element size of 0.8 mm was selected (~14,000,000 elements) based on a grid independence study; in addition, the initial tetrahedral mesh was converted to a polyhedral mesh before performing CFD simulations.[24] Boundary conditions (BCs) necessary to run the computational simulations were extracted from echocardiographic data. Briefly, 0-gauge pressure inlet BCs were applied

at the pulmonary veins and a time-dependent velocity waveform from the MV (V_{out}), which matched the rhythm of each patient, was applied at the outlet (**Figure 1**). These BCs were in accordance with our previous work and similar published studies in literature.[24,25] CFD simulations were performed using Ansys Fluent and based on the finite volume approach to discretize the Navier-Stokes equations (Supplemental Appendix). Blood was simulated as an incompressible Newtonian fluid with a density $\rho = 1{,}060\ kg/m^3$ and a dynamic viscosity $\mu = 0.0035$ Pa s. Because the Reynolds number, estimated from peak MV at the E-wave and the MV diameter, was <2000 in all cases, a laminar model was chosen. This was also in accordance with other studies in literature.[24,25] Three cycles of a transient simulation were carried out to ensure stability and to overcome transitional effects.[23,25] For data analysis, the final cycle was used for stability.

FLOW DYNAMIC PARAMETERS. Nonphysiological levels of wall shear stress (WSS) have been associated with platelet and endothelial cell activation resulting in thrombogenesis.[26] In this study, we computed several flow dynamic parameters with WSS as a function. This includes time averaged wall shear stress (TAWSS), oscillatory shear index (OSI), and endothelial cell activation potential (ECAP). The derivations for each parameter are listed in the Supplemental Appendix.

TAWSS is the average WSS over the cardiac cycle. Averaging the change in WSS across the cardiac cycle may highlight regions of nonphysiological WSS levels, which might in turn, be associated with thrombogenesis.[27] *OSI* describes the deflection (change in direction) of the WSS vectors from the main flow direction throughout a cardiac cycle.[28] OSI has an interval of 0 to 0.5, where 0 and 0.5 indicate no deflection and a deflection of 180°, respectively. Regions of high OSI have been shown to induce an inflammatory response,[27] promoting thrombogenesis as described within the triad of Virchow.[29] *ECAP* consists of the ratio between OSI and TAWSS. It has been proposed as a useful flow dynamic parameter as it may be utilized for identifying vasculature with a higher possibility of thrombogenesis.[30] A high ECAP indicates low TAWSS and high OSI, which have been shown to be associated with thrombogenesis.[27]

STATISTICS. Statistical analysis was performed using JMP Pro, version16.0.0 (SAS Institute Inc). All data are presented as mean ± SD. A *t*-test test was used to compare the means (if the distribution was normal) and the Wilcoxon test was used for non-normal data distributions. $P < 0.05$ was considered statistically significant. Statistical analysis was conducted on the value taken from the nodal elements of each patient's device, resulting in tens of thousands of data points for both groups while verifying the normality assumption.

TABLE 1 Patient Characteristics

	DRT (n = 19)	Control (n = 19)	*P* Value
Age >75 (y)	8 (42.1%)	9 (47.4%)	0.6550
Male	14 (73.7%)	10 (52.6%)	0.1902
BMI	29.2 ± 6.3	26 ± 5.2	0.0932
CHA2DS2-VASc	4.1 ± 1.2	4.4 ± 1.7	0.5902
Has bled score	3 ± 0.9	2.7 ± 1.3	0.3547
AF type			0.3253
Paroxysmal	8 (42.1%)	12 (63.2%)	
Permanent	10 (52.6%)	5 (26.3%)	
Unspecified	1 (5.3%)	2 (10.5%)	
History			
Heart failure	5 (26.3%)	4 (21.1%)	0.7213
Diabetes	6 (31.6%)	3 (15.8%)	0.2671
Ischemic stroke or TIA	6 (31.6%)	5 (26.3%)	0.7381
Other vascular disease	7 (36.8%)	4 (21.1%)	0.2982
Hypertension	15 (78.9%)	13 (68.4%)	0.4790
Abnormal liver function	0 (0%)	0 (0%)	1.0000
Abnormal renal function	5 (26.3%)	8 (42.1%)	0.3200
Ischemic heart disease	9 (47.4%)	8 (42.1%)	0.7604
PCI	5 (26.3%)	4 (21.1%)	0.7213
CABG	4 (21.1%)	1 (5.3%)	0.1628
LVEF (%)	55.7 ± 5.1	54 ± 10.3	0.6774
Valvular heart disease	3 (15.8%)	5 (26.3%)	0.4445
CRT/pacemaker/ICD	2 (10.5%)	3 (15.8%)	0.6537
Indications			
Intracranial hemorrhage	6 (31.6%)	3 (15.8%)	0.2671
GI bleed	5 (26.3%)	5 (26.3%)	1.0000
Urinary tract bleeding	0 (0%)	0 (0%)	1.0000
Other spontaneous bleeding	1 (5.3%)	2 (10.5%)	0.5739
Stroke despite OAC	5 (26.3%)	5 (26.3%)	1.0000
Cerebral amyloid angiopathy	0 (0%)	2 (10.5%)	0.1627
Cognitive impairment	3 (15.8%)	0 (0%)	0.0802
Patient preference/lack of compliance/side effects	7 (36.8%)	5 (26.3%)	0.5025
Device size			0.6530
20 mm	1 (5.3%)	0 (0%)	
22 mm	0 (0%)	1 (5.3%)	
24 mm	0 (0%)	2 (10.5%)	
25 mm	2 (10.5%)	0 (0%)	
27 mm	10 (52.6%)	7 (36.8%)	
30 mm	0 (0%)	1 (5.3%)	
31 mm	4 (21.1%)	7 (36.8%)	
34 mm	1 (5.3%)	0 (0%)	
35 mm	1 (5.3%)	1 (5.3%)	
Device type			
WATCHMAN	1 (5.3%)	3 (15.8%)	
WATCHMAN FLX	14 (73.7%)	13 (68.4%)	
Amplatzer Amulet	4 (21.1%)	3 (15.8%)	
Discharge antithrombotics			

Continued on the next page

TABLE 1 Continued

	DRT (n = 19)	Control (n = 19)	*P* Value
Acetylsalicylic acid (ASA) therapy (aspirin)	16 (84.2%)	14 (73.7%)	0.4445
P2Y12-inhibitor (clopidogrel, ticagrelor, etc.)	8 (42.1%)	9 (47.4%)	0.7604
Vitamin K antagonist (VKA) (warfarin)	2 (10.5%)	3 (15.8%)	0.6537
DOAC (apixaban, rivaroxaban, edoxaban, dabigatran)	4 (21.1%)	4 (21.1%)	1.0000
Low-molecular-weight heparin (LMWH)	0 (0%)	0 (0%)	1.0000
No antithrombotic therapy	0 (0%)	0 (0%)	1.0000
Time from follow-up (LAAO to post-CT)	112.5 ± 118	105.8 ± 108.4	0.8100

Values are n (%) or mean ± SD.

AF = atrial fibrillation; CABG = coronary artery bypass graft surgery; CRT = cardiac resynchronization therapy; CT = computed tomography; DOAC = direct oral anti-coagulation; DRT = device-related thrombosis; GI = gastrointestinal; ICD = implantable cardioverter-defibrillator; LAAO = left atrial appendage occlusion; LVEF = left ventricular ejection fraction; OAC = oral anti-coagulation; P2Y12 = purinergic receptor P2Y, G-protein coupled, 12 protein; PCI = percutaneous coronary intervention; TIA = transient ischemic attack.

RESULTS

TIME AVERAGED WALL SHEAR STRESS. The TAWSS contour plots are shown in Supplemental Figure 2; only the portion of the device exposed to the atrial flow is shown. To quantify the differences between patient populations, **Table 2** shows a global account of the TAWSS values and **Figure 2A** shows a sample of contours. The mean TAWSS was found to be 1.76 ± 1.24 Pa for the DRT cohort and 2.90 ± 2.70 Pa for the control cohort with $P < 0.0001$.

OSCILLATORY SHEAR INDEX. The OSI contour plots are shown in Supplemental Figure 3; only the portion of the device exposed to the atrial flow is shown. To quantify the differences between patient populations, **Table 2** shows a global account of the OSI values and **Figure 2B** shows a sample of contours. The mean OSI was found to be 0.19 ± 0.11 for the DRT cohort and 0.17 ± 0.11 for the control cohort with $P < 0.0001$.

ENDOTHELIAL CELL ACTIVATION POTENTIAL. The ECAP contour plots are shown in Supplemental Figure 4; only the portion of the device exposed to the atrial flow is shown. To quantify the differences between patient populations, **Table 2** shows a global account of the ECAP values and **Figure 2C** shows a sample of contours. The mean ECAP was found to be 0.23 ± 0.58 Pa^{-1} for the DRT cohort and 0.17 ± 0.30 Pa^{-1} for the control cohort with $P < 0.0001$.

THROMBUS LOCATION AND VOLUME FROM IN-VIVO IMAGING. The boundaries of the thrombi found in each DRT patient's post-CT scan are overlayed for each flow dynamic parameter (Supplemental Figures 2 to 4). The thrombi were mainly observed in regions of low WSS, high OSI, and high ECAP. The total mean volume of the thrombi was 1.44 ± 2.06 mL (**Table 2**).

GEOMETRIC MEASUREMENTS. Measurements of the LA volume and MV area are shown in **Table 2**. Mean LA volume was larger among the DRT cohort compared with the controls (171.49 ± 69.16 mL and 127.90 ± 33.82 mL, respectively; $P < 0.05$). Also, the mean MV area was larger for the DRT cohort (1,340.64 ± 401.37 mm^2 and 1,061.89 ± 380.07 mm^2, respectively; $P < 0.05$).

DISCUSSION

This study represents the most comprehensive assessment to identify flow dynamics patterns that correlate with DRT to date. Using a novel approach that combined patient-specific modeling with CFD and finite element simulations to obtain a more realistic patient-specific and device deformation, we documented a strong association between certain flow parameters and DRT. Accordingly, patients with clinically adjudicated DRT displayed lower TAWSS, higher OSI, and higher ECAP than controls ($P < 0.001$ for all), supporting existing pathophysiological concepts. This computational approach approximates a realistic model for assessing flow dynamics in relation to DRT and represents a step forward in the growing trends to incorporate computational simulations in the planning of LAAO procedures.

Endothelial cell dysfunction is a known predictor of thrombus formation.[26,31,32] Numerous studies have explored WSS as a possible factor in endothelial dysfunction,[26,31,33] particularly noting the association of low WSS levels with thrombogenesis.[27,34] In line with these previous findings, our study shows that DRT patients had a lower TAWSS compared to the controls. A low TAWSS indicates a region of blood stasis, which can induce thrombosis due to the accumulation of procoagulant components.[35] Furthermore, our study documented that DRT was mainly located within or close by to regions with low levels of TAWSS. These lower TAWSS values may be related to device deployment. Zhong et al[18] have shown that a deep device deployment depth resulted in lower TAWSS whereas a device deployed at the LAA ostium was higher. Clinical studies have also shown a higher incidence of DRT with deeper device deployments.[36,37] When the device is deployed deep into the LAA, a shallow "valley" is created above the device that serves as a nidus for blood stagnation and thrombus formation. The larger atrial volumes and MV areas observed in the DRT patients might lead to lower velocities, ultimately yielding an increased risk of flow stagnation and thrombus formation.

FIGURE 1 Workflow Adopted for This Study, Utilizing a Sequence of Finite Element Analysis and Computational Fluid Dynamics

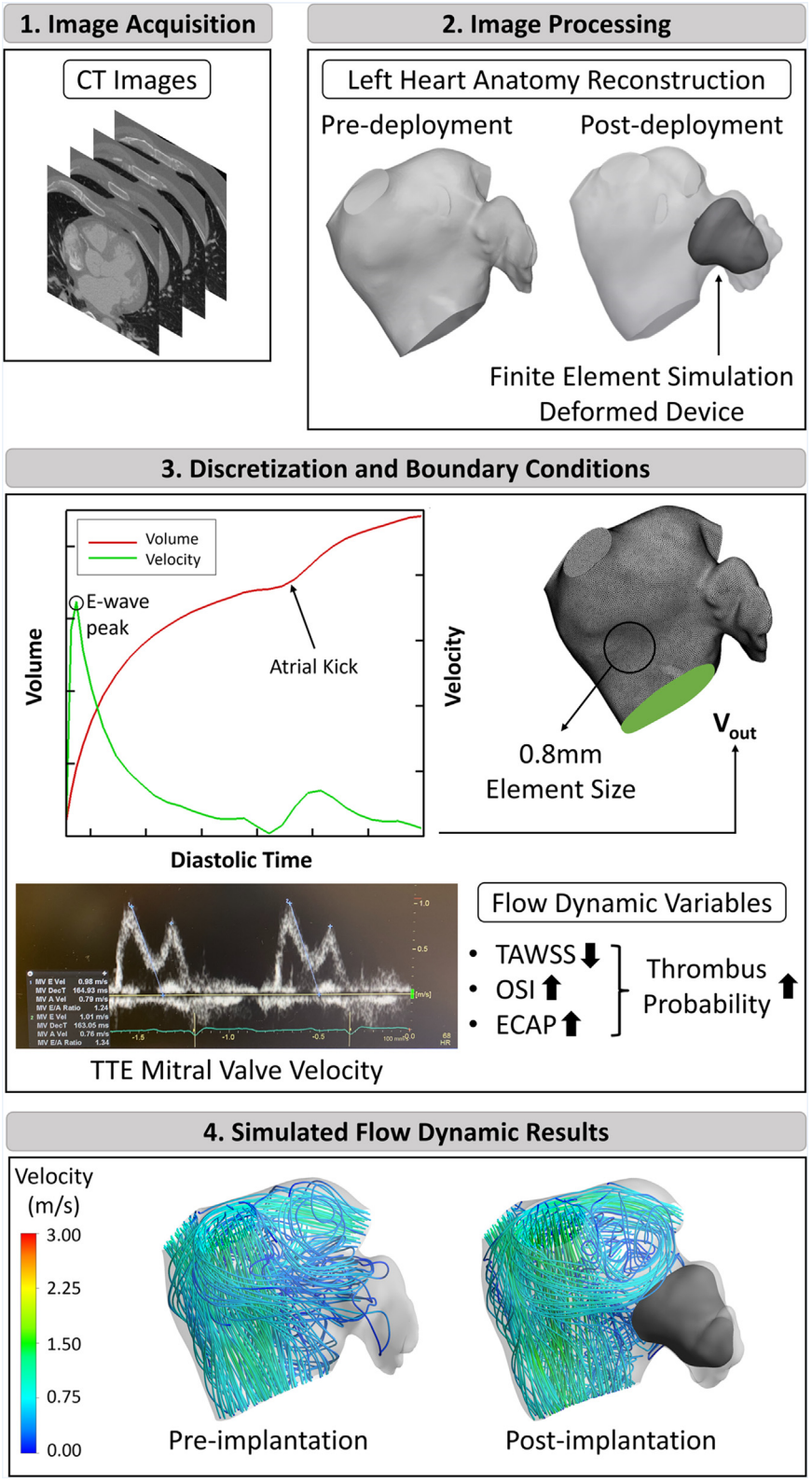

CT = computed tomography; ECAP = endothelial cell activation potential; OSI = oscillatory shear index; TAWSS = time averaged wall shear stress; TTE = transthoracic echocardiogram.

TABLE 2 Flow Dynamics Metrics and Geometric Measurements of Device-Related Thrombosis and Control Patients

	Group	Mean	Median	SD	IQR	*P* Value
Flow dynamics metrics						
TAWSS (Pa)	DRT	1.76	1.43	1.24	1.42	<0.0001
	CTL	2.90	2.14	2.70	2.86	
OSI	DRT	0.19	0.17	0.11	0.17	<0.0001
	CTL	0.17	0.15	0.11	0.17	
ECAP (Pa^{-1})	DRT	0.23	0.12	0.58	0.20	<0.0001
	CTL	0.17	0.07	0.30	0.15	
Geometric measurements						
Left atrium volume (mL)	DRT	171.49	143.11	69.16	88.91	<0.05
	CTL	127.90	127.36	33.82	61.30	
Mitral valve area (mm^2)	DRT	1,340.64	1,309.88	401.37	573.25	<0.05
	CTL	1,061.89	963.94	380.07	491.83	
Thrombus volume (mL)	DRT	1.44	0.53	2.06	1.72	

Low TAWSS, high OSI, and high ECAP are associated with thrombosis.

CTL = control; DRT = device-related thrombosis; ECAP = endothelial cell activation potential; OSI = oscillatory shear index; TAWSS = time averaged wall shear stress.

Another important flow dynamic parameter investigated was OSI. Oscillatory flow can promote an inflammatory state which can result in endothelial cell dysfunction, a potential nidus for thrombus formation.[27,32] The presence of an LAAO device may influence the flow patterns within the atrium, potentially resulting in increased oscillatory shear. In the case of a deeper device deployment, a recirculation region develops on top of the device increasing the oscillatory shear around the device.[38,39] In this study, the DRT cohort was observed to have higher OSI than the controls. In addition, there was a correlation between the location of the thrombus identified from in-vivo imaging and regions of high OSI. Although not seen in this study, residual (micro) peri-device leaks may also influence OSI.

ECAP has been shown in various studies to confer areas of susceptibility at the vessel walls.[18,30,40,41] ECAP is defined as the ratio of OSI and TAWSS, where a high value indicates a high OSI and a low TAWSS, both of which have been shown to be related to thrombogenesis. Endothelial cells naturally provide an antithrombotic surface,[32,42] but when activated, this property is negated, which can result in thrombus formation.[32,35] In this study, we observed an elevated ECAP for the DRT cohort compared to the controls further confirming the potential role of CFD parameters in predicting DRT.

Our findings have important practical implications. Mitigating the occurrence of DRT remains a key challenge in LAAO. The first step to address this problem is to understand the possible causes and to identify potential predictors of DRT. Clinical studies attempted to identify predictors of DRT but studies identifying risk factors did not account for flow dynamics, despite DRT being pathophysiologically intimately related to flow patterns. Therefore, our study provides a comprehensive understanding and characterization of the flow environment around the LAAO device to see what the differences are between patients with DRT and without DRT. Our study provides evidence that certain flow parameters (lower TAWSS, higher OSI, and higher ECAP) are associated with DRT. This information may, in time: 1 help estimate the likelihood of DRT prior to LAAO, guiding shared decision-making and improving appropriate patient selection; and 2) assist the design of future research to assess whether a tailored device implant or positioning might further mitigate the risk of DRT in patient-specific anatomies.

The uniqueness of this work stems from combining the finite element with the CFD approach, while implementing the deformation of the atrium and the device after deployment. In addition, this work involves a unique data set of LAAO patients who developed DRT with full imaging from three different medical institutions.

STUDY LIMITATIONS. The cohort used included only 19 individuals in each group. A larger patient population may help to better identify the threshold for each parameter studied associated with DRT. In addition, the study did not employ fluid structure interaction analysis, which might improve reproducibility of the LA flow dynamics. Due to CT quality and limitations in the FE process, not all patients are matched by age and sex. Therefore, we have opted to show a global comparison between the two groups as opposed to a direct comparison of each patient.

CONCLUSIONS

In this comprehensive study of flow dynamics in patients undergoing LAAO, we documented a characteristic flow profile in patients with DRT (low TAWSS, high OSI, and high ECAP) as compared with controls. Our novel approach combining CFD assessment with finite element simulations may improve risk stratification among patients referred for LAAO (**Central Illustration**). Further research involving a larger patient cohort and long-term follow-up is necessary to understand the impact of the routine evaluation of flow dynamic parameters on risk stratification of LAAO candidates.

FIGURE 2 Sample of TAWSS, OSI, and ECAP Contours for the Top Surface of Each Device for the DRT and CTL Populations

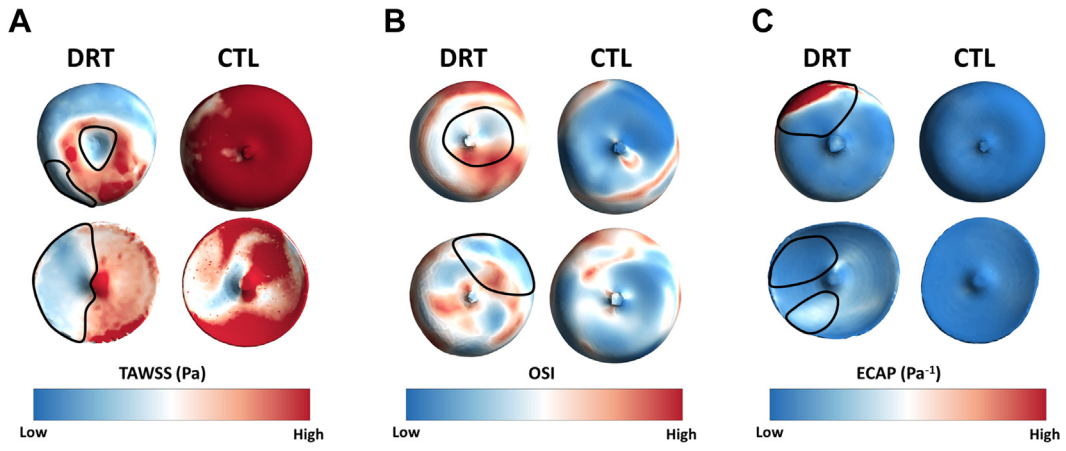

Sample of time averaged wall shear stress (A), oscillatory shear index (B), and endothelial cell activation potential (C) contours for the top surface of each device for the device-related thrombosis, and control populations. Thrombus locations from in-vivo imaging are shown by the black line for each drt patient displayed. The line represents the border of the thrombus. DRT = device-related thrombosis; CTL = control; other abbreviations as in Figure 1.

CENTRAL ILLUSTRATION Flow Dynamic Factors Correlated With Device-Related Thrombosis After Left Atrial Appendage Occlusion

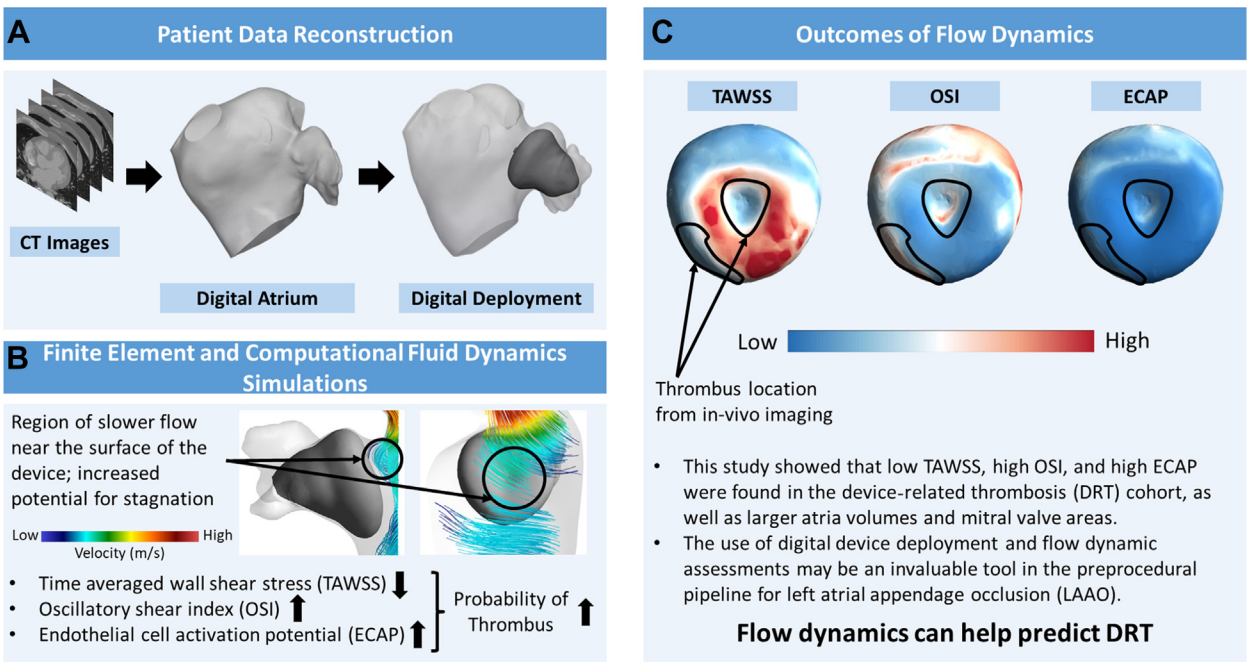

Vogl BJ, et al. JACC Adv. 2024;3(11):101339.

Patient-specific modeling (A) of the left atrium and left atrial appendage occlusion devices for use in a combined finite element and computational fluid dynamics simulations (B) to identify fluid dynamics predictors of device related thrombosis (DRT). (C) Patients with DRT had lower time averaged wall shear stress, high oscillatory shear index, and high endothelial cell activation potential, indicating an increased likelihood of thrombosis. ECAP = endothelial cell activation potential; OSI = oscillatory shear index; TAWSS = time averaged wall shear stress; abbreviations as in Figures 1 and 2.

FUNDING SUPPORT AND AUTHOR DISCLOSURES

This research was partly supported by the American Heart Association (AHA) under award number 24CDA1269661. Dr De Backer has received consulting fees and institutional research grants from Abbott and Boston Scientific. Dr Nielsen-Kudsk has received institutional research grants from Abbott, Boston Scientific, and the Novo Nordic Foundation. Dr Bavo is an employee of FEops. Dr De Beule is a shareholder of FEops. Dr Vogl was partially supported by the Blue Cross Blue Shield of Michigan Foundation, the DeVlieg Foundation, and the Health Research Institute fellowship at Michigan Tech. Dr Jia has received a scholarship from China Scholarship Council under the State Scholarship Fund of China. All other authors have reported that they have no relationships relevant to the contents of this paper to disclose.

ADDRESS FOR CORRESPONDENCE: Prof Hoda Hatoum, Michigan Technological University, Department of Biomedical Engineering, 1400 Townsend Dr, Houghton, Michigan 49931, USA. E-mail: hhatoum@mtu.edu. OR Dr Mohamad Alkhouli, Mayo Clinic, 200 First Street SW, Rochester, Minnesota 55905, USA. E-mail: Alkhouli.Mohamad@mayo.edu.

PERSPECTIVES

COMPETENCY IN MEDICAL KNOWLEDGE: In this analysis, we demonstrated through a combined finite element analysis and computational fluid dynamic approach—where the device and LAA deformation were replicated similar to in-vivo—that patients with DRT exhibit larger LA volumes and MV areas in addition to more elevated oscillatory shear and ECAP combined with lower shear stress. The location of the thrombi verified the hemodynamic findings.

TRANSLATIONAL OUTLOOK: Further research involving a larger patient cohort and long-term follow-up is necessary to understand the impact of the routine evaluation of flow dynamic parameters on risk stratification of LAAO candidates.

REFERENCES

1. Kornej J, Börschel CS, Benjamin EJ, Schnabel RB. Epidemiology of atrial fibrillation in the 21st century: novel methods and new insights. *Circ Res*. 2020;127:4–20.

2. Reddy VY, Doshi SK, Kar S, et al. 5-year outcomes after left atrial appendage closure: from the PREVAIL and PROTECT AF trials. *J Am Coll Cardiol*. 2017;70:2964–2975.

3. Alkhouli M, Ellis CR, Daniels M, Coylewright M, Nielsen-Kudsk JE, Holmes DR. Left atrial appendage occlusion: current advances and remaining challenges. *JACC Adv*. 2022:100136.

4. Holmes DR Jr, Alkhouli M, Reddy V. Left atrial appendage occlusion for the unmet clinical needs of stroke prevention in nonvalvular atrial fibrillation. *Mayo Clin Proc*. 2019;94:864–874.

5. Alkhouli M, Alqahtani F, Aljohani S, Alvi M, Holmes DR. Burden of atrial fibrillation-associated ischemic stroke in the United States. *JACC Clin Electrophysiol*. 2018;4:618–625.

6. Bshennaty A, Vogl BJ, Bavo AM, et al. Understanding the role of the left atrial appendage on the flow in the atrium. *Catheter Cardiovasc Interv*. 2024. https://doi.org/10.1002/ccd.31153

7. Alkhouli M, Ellis CR, Daniels M, Coylewright M, Nielsen-Kudsk JE, Holmes DR. Left atrial appendage occlusion. *JACC Adv*. 2022;1:100136.

8. Alkhouli M, Busu T, Shah K, Osman M, Alqahtani F, Raybuck B. Incidence and clinical impact of device-related thrombus following percutaneous left atrial appendage occlusion: a meta-analysis. *JACC Clin Electrophysiol*. 2018;4:1629–1637.

9. Simard TJ, Hibbert B, Alkhouli MA, Abraham NS, Holmes DR Jr. Device-related thrombus following left atrial appendage occlusion. *Eurointervention*. 2022;18(3):224–232.

10. Holmes DR Jr, Korsholm K, Rodes-Cabau J, Saw J, Berti S, Alkhouli MA. Left atrial appendage occlusion. *EuroIntervention*. 2023;18:e1038–e1065.

11. Kramer AD, Korsholm K, Jensen JM, et al. Cardiac computed tomography following Watchman FLX implantation: device-related thrombus or device healing? *Eur Heart J Cardiovasc Imaging*. 2023;24:250–259.

12. Sedaghat A, Nickenig G, Schrickel JW, et al. Incidence, predictors and outcomes of device-related thrombus after left atrial appendage closure with the WATCHMAN device—insights from the EWOLUTION Real World Registry. *Cathet Cardiovasc Interv*. 2021;97:E1019–E1024.

13. Mesnier J, Simard T, Jung RG, et al. Persistent and recurrent device-related thrombus after left atrial appendage closure: incidence, predictors, and outcomes. *JACC Cardiovasc Interv*. 2023;16:2722–2732.

14. Alkhouli M, Alarouri H, Kramer A, et al. Device-related thrombus after left atrial appendage occlusion: clinical impact, predictors, classification, and management. *JACC Cardiovasc Interv*. 2023;16:2695–2707.

15. Vogl B, El Shaer A, Ponce AC, et al. TCT-380 predicting device-related thrombosis using computational fluid dynamics. *J Am Coll Cardiol*. 2022;80:B153.

16. Lowe GD. Virchow's triad revisited: abnormal flow. *Pathophysiol Haemost Thromb*. 2003;33:455–457.

17. Alkhouli M, Hatoum H, Piazza N. Computational modeling to guide structural Heart interventions: measure twice (or thrice) but cut once. *JACC Cardiovasc Interv*. 2023;16:667–669.

18. Zhong Z, Gao Y, Kovács S, et al. Impact of left atrial appendage occlusion device position on potential determinants of device-related thrombus: a patient-specific in silico study. *Clin Res Cardiol*. 2023;113(10):1405–1418.

19. Aguado AM, Olivares AL, Yagüe C, et al. In silico optimization of left atrial appendage occluder implantation using interactive and modeling tools. *Front Physiol*. 2019;10:237.

20. Mill J, Agudelo V, Olivares AL, et al. Sensitivity analysis of in silico fluid simulations to predict thrombus formation after left atrial appendage occlusion. *Mathematics*. 2021;9:2304.

21. Bavo AM, Wilkins BT, Garot P, et al. Validation of a computational model aiming to optimize preprocedural planning in percutaneous left atrial appendage closure. *J Cardiovasc Comput Tomogr*. 2020;14:149–154.

22. D'Alessandro N, Falanga M, Masci A, Severi S, Corsi C. Preliminary findings on left atrial appendage occlusion simulations applying different endocardial devices. *Front Cardiovasc Med*. 2023;10:1067964.

23. Trusty PM, Wei ZA, Fogel MA, Maher K, Deshpande SR, Yoganathan AP. Computational Modeling of a right-sided Fontan assist device: effectiveness across patient anatomies and cannulations. *J Biomech*. 2020;109:109917.

24. Vogl BJ, Shaer AE, Van Zyl M, Killu AM, Alkhouli M, Hatoum H. Effect of catheter ablation

on the hemodynamics of the left atrium. *J Intervent Card Electrophysiol*. 2022;65:83-96.

25. Bosi GM, Cook A, Rai R, et al. Computational fluid dynamic analysis of the left atrial appendage to predict thrombosis risk. *Front Cardiovasc Med*. 2018;5:34.

26. Chiu J-J, Chien S. Effects of disturbed flow on vascular endothelium: pathophysiological basis and clinical perspectives. *Physiol Rev*. 2011;91:327-387.

27. Hathcock JJ. Flow effects on coagulation and thrombosis. *Arterioscler Thromb Vasc Biol*. 2006;26:1729-1737.

28. Soulis JV, Lampri OP, Fytanidis DK, Giannoglou GD. *Relative Residence Time and Oscillatory Shear Index of Non-Newtonian Flow Models in Aorta*. 2011 10th International Workshop on Biomedical Engineering; 2011.

29. Esmon CT. Inflammation and thrombosis. *J Thromb Haemostasis*. 2003;1:1343-1348.

30. Di Achille P, Tellides G, Figueroa CA, Humphrey JD. A haemodynamic predictor of intraluminal thrombus formation in abdominal aortic aneurysms. *Proc R Soc A*. 2014;470:20140163.

31. Chien S. Effects of disturbed flow on endothelial cells. *Ann Biomed Eng*. 2008;36:554-562.

32. Yau JW, Teoh H, Verma S. Endothelial cell control of thrombosis. *BMC Cardiovasc Disord*. 2015;15:130.

33. Hyun S, Kleinstreuer C, Archie JP Jr. Hemodynamics analyses of arterial expansions with implications to thrombosis and restenosis. *Med Eng Phys*. 2000;22:13-27.

34. Buck AKW, Groszek JJ, Colvin DC, et al. Combined in silico and in vitro approach predicts low wall shear stress regions in a hemofilter that correlate with thrombus formation in vivo. *ASAIO J*. 2018;64:211-217.

35. Mackman N. New insights into the mechanisms of venous thrombosis. *J Clin Invest*. 2012;122:2331-2336.

36. Cepas-Guillén P, Flores-Umanzor E, Leduc N, et al. Impact of device implant depth after left atrial appendage occlusion. *JACC Cardiovasc Interv*. 2023;16:2139-2149.

37. Sedaghat A, Vij V, Al-Kassou B, et al. Device-related thrombus after left atrial appendage closure: data on thrombus characteristics, treatment strategies, and clinical outcomes from the EUROC-DRT-registry. *Circ Cardiovasc Interv*. 2021;14:e010195.

38. DiCarlo AL, Holdsworth DW, Poepping TL. Study of the effect of stenosis severity and non-Newtonian viscosity on multidirectional wall shear stress and flow disturbances in the carotid artery using particle image velocimetry. *Med Eng Phys*. 2019;65:8-23.

39. Compagne KCJ, Dilba K, Postema EJ, et al. Flow patterns in carotid webs: a patient-based computational fluid dynamics study. *AJNR Am J Neuroradiol*. 2019;40:703-708.

40. García-Isla G, Olivares AL, Silva E, et al. Sensitivity analysis of geometrical parameters to study haemodynamics and thrombus formation in the left atrial appendage. *Int J Numer Method Biomed Eng*. 2018;34:e3100.

41. Paliwal N, Ali RL, Salvador M, et al. Presence of left atrial fibrosis may contribute to aberrant hemodynamics and increased risk of stroke in atrial fibrillation patients. *Front Physiol*. 2021;12:657452.

42. Neubauer K, Zieger B. Endothelial cells and coagulation. *Cell Tissue Res*. 2022;387:391-398.

KEY WORDS **device-related thrombosis, DRT, LAAO, left atrial appendage occlusion, thrombosis**

APPENDIX **For supplemental information and figures, please see the online version of this paper.**